7-16-2012

Absolute Properties of the Eclipsing Binary Star V335 Serpentis

Claud H. Sandberg Lacy
University of Arkansas, Fayetteville

Francis C. Fekel
Tennessee State University

Antonio Claret
Instituto de Astrofisica de Andalucia

The Astronomical Journal, 144:63 (8pp), 2012 August doi:10.1088/0004-6256/144/2/63

ABSOLUTE PROPERTIES OF THE ECLIPSING BINARY STAR V335 SERPENTIS

Claud H. Sandberg Lacy[1,4], Francis C. Fekel[2,4,5], and Antonio Claret[3]
[1] Physics Department, University of Arkansas, Fayetteville, AR 72701, USA; clacy@uark.edu
[2] Center of Excellence in Information Systems, Tennessee State University, Nashville, TN 37209, USA; fekel@evans.tsuniv.edu
[3] Instituto de Astrofisica de Andalucia, CSIC, Apdo. Postal 3004, E-18080 Granada, Spain; claret@iaa.es
Received 2012 May 25; accepted 2012 June 22; published 2012 July 16

ABSTRACT

V335 Ser is now known to be an eccentric double-lined A1+A3 binary star with fairly deep (0.5 mag) partial eclipses. Previous studies of the system are improved with 7456 differential photometric observations from the URSA WebScope and 5666 from the NFO WebScope, and 67 high-resolution spectroscopic observations from the Tennessee State University 2 m automatic spectroscopic telescope. From dates of minima, the apsidal period is about 880 years. Accurate (better than 2%) masses and radii are determined from analysis of the two new light curves and the radial velocity curve. Theoretical models match the absolute properties of the stars at an age of about 380 Myr, though the age agreement for the two components is poor. Tidal theory correctly confirms that the orbit should still be eccentric, but we find that standard tidal theory is unable to match the observed asynchronous rotation rates of the components' surface layers.

Key words: binaries: eclipsing – binaries: spectroscopic – stars: fundamental parameters – stars: individual (V335 Ser)

Online-only material: machine-readable and VO tables

1. INTRODUCTION

Eclipsing binary stars provide critical information that can be used to test our current theories of stellar evolution. By measuring accurately the changes in brightness over time (the light curve), times of minimum light (the ephemeris curve), and the pattern of changing radial velocities of the components (the radial velocity curve), orbital parameters may be determined including the masses, radii, luminosities, and internal structure constant. Additionally, the projected rotation rates ($v \sin i$) of the components may be measured from high-resolution spectra. These observationally determined values can then be compared with theoretical results from the current theory of stellar evolution to gauge the degree of completeness of the theory. These are the main goals of this type of investigation. A general compilation and investigation of the results from these types of studies is given by Torres et al. (2010).

The detached eccentric main-sequence eclipsing binary star V335 Ser (BD+01 3151, HD 143213, SAO 121294, TYC 353–301-1) is a relatively bright star ($V = 7.45$ mag), originally classified as spectral type A0 but now known to be A1+A3. It was first discovered as a variable star from measurements by the TYCHO instrument of the *Hipparcos* satellite (Makarov et al. 1994). Bastian & Born (1997, 1998) determined the first accurate eclipse ephemeris, with a period of about 3.45 days. This star was classified as a spectral class A1 spectroscopic binary by Paunzen et al. (2001). The displacement of the secondary eclipse indicated an eccentric orbit, and many times of minima have been published (see Section 2). Bozkurt (2011) was the first to report absolute properties of this system, based on many fewer observations than ours, but his results differ significantly from ours.

2. PRIMARY ECLIPSE EPHEMERIS

Published photoelectric or CCD dates of minima have been gathered and are given in Table 1. In cases where multiple observations were made of the same eclipse in different filters with the same equipment, a mean value is cited in Table 1 with an uncertainty reflecting the scatter of values published. A linear ephemeris was fitted to the dates of primary eclipse by using a least-squares method that scaled the uncertainties to produce a reduced chi-square of unity, which is necessary to accurately calculate the uncertainties of the period and zero epoch. The results, based on the 13 dates of primary minima, are HJD Min $I = 2{,}454{,}685.70124(18)+3.4498837(12)\ E$.

Residuals are shown in Figure 1. This ephemeris was used in analyzing the photometry and radial velocities to be discussed below.

3. APSIDAL MOTION

An ephemeris curve solution was made by using the least-squares method of Lacy (1992) on the data in Table 1. This method allows one to accurately estimate many of the orbital parameters of the binary star and their uncertainties by using an iterated least-squares fitting algorithm applied to the observed dates of minima, taking into account the published observational errors. The principal orbital parameters determined from fitting this so-called ephemeris curve are the eccentricity (e), anomalistic period (P_a), longitude of periastron (ω), apsidal motion rate ($\dot{\omega}$), and reference time of minimum light (T_o). These five parameters are fitted to the data. The inclination was fixed at the value found in the photometric solution (see Section 5). The apsidal motion period (U) can be calculated easily from the apsidal motion rate. Apsidal motion in this binary system is due to both a classical Newtonian interaction and the general relativistic

[4] Visiting Astronomer, Kitt Peak National Observatory, National Optical Astronomy Observatories, operated by the Association of Universities for Research in Astronomy, Inc., under a cooperative agreement with the National Science Foundation.
[5] The research at Tennessee State University was supported in part by NASA, NSF, Tennessee State University, and the state of Tennessee through its Centers of Excellence program.

Table 1
Times of Eclipse of V335 Ser and Residuals from the Ephemeris Curve Fit

Year	HJD−2400000	Precision (days)	Cycle Number	Eclipse Type	$O-C$ (days)	Method	Ref.
2000.4	51708.44940	0.0020	−863	1	−0.00222	pe	1
2006.4	53885.32840	0.0003	−232	1	0.00023	pe	2
2006.5	53911.33990	0.0018	−225	2	0.00006	pe	2
2006.6	53942.38830	0.0012	−216	2	−0.00032	pe	2
2007.5	54287.37570	0.0007	−116	2	0.00066	pe	2
2007.5	54292.41460	0.0002	−114	1	0.00016	pe	2
2008.4	54599.45400	0.0005	−25	1	−0.00009	pe	3
2008.4	54616.70310	0.0002	−20	1	−0.00040	pe	4
2008.4	54616.70320	0.0002	−20	1	−0.00030	pe	4
2008.6	54670.31630	0.0034	−5	2	0.00635	pe	2
2008.6	54675.35250	0.0002	−3	1	0.00097	pe	2
2010.3	55299.77950	0.0003	178	1	−0.00098	pe	5
2010.4	55337.72900	0.0002	189	1	−0.00020	pe	5
2010.5	55368.77760	0.0004	198	1	−0.00056	pe	5
2010.5	55384.43780	0.0006	202	2	0.00599	pe	2
2010.5	55396.37870	0.0004	206	1	0.00147	pe	2
2010.6	55401.67900	0.0003	207	2	−0.00213	pe	5
2010.7	55451.57510	0.0006	222	1	−0.00026	pe	5
2011.2	55630.96970	0.0002	274	1	0.00038	pe	6
2011.4	55694.92120	0.0005	292	2	0.00163	pe	6

Note. [a] Eclipses of type 1 are the deeper eclipses when the hotter, more massive component (star A) is being eclipsed by the cooler, less massive component (star B).
References: (1) Agerer & Hübscher 2002; (2) Bozkurt 2011; (3) Brat et al. 2008; (4) Lacy 2009; (5) Lacy 2011; (6) Lacy 2012.

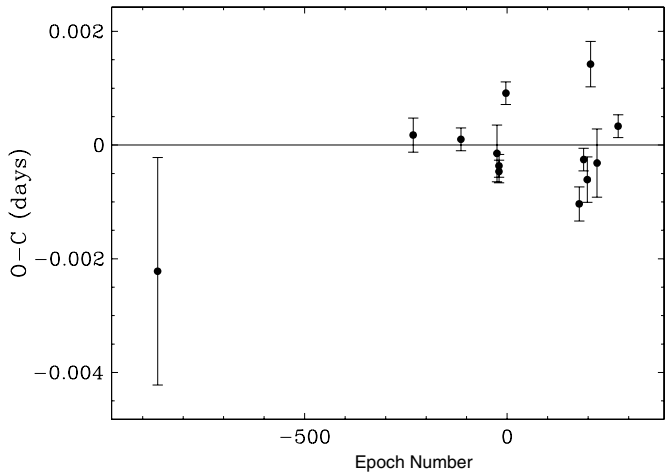

Figure 1. Residuals from a linear ephemeris fitted to published photoelectric or CCD dates of primary eclipse of V335 Ser.

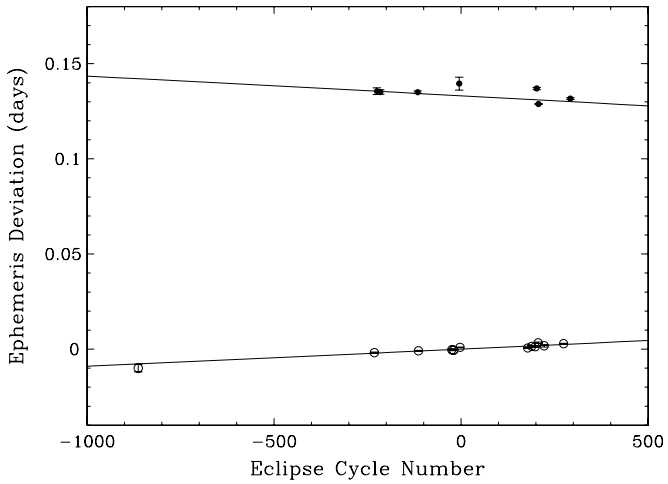

Figure 2. Ephemeris curve fit to the photoelectric or CCD dates of primary eclipse (open circles) and secondary eclipse (filled circles) of V335 Ser. The observations cover about 10 years. The full apsidal period U is about 880 years.

effect, but the Newtonian contribution is the greater one in this case, being five times as large as the relativistic contribution.

Uncertainties in the dates of minima were adjusted (scaled) by the fitting method in order to result in a reduced chi-square of unity, which is a necessary step for the accurate estimation of the fitted orbital parameter uncertainties via the Levenberg–Marquardt method. The orbital parameters so determined are given in Table 2, and the fit is displayed in Figure 2. No noticeable pattern is evident in the residuals to the fit, which fact is consistent with the assumption that the binary system does not appear to have any additional close stellar components.

4. SPECTROSCOPIC OBSERVATIONS AND ORBIT

At Fairborn Observatory from 2010 February through 2011 June we acquired 67 double-lined spectra with the Tennessee

Table 2
Orbital Parameters Derived from or Assumed in Fits to the Dates of Minimum Light

Parameters	Fitted Values
e	0.1443 ± 0.0025
P_a (days)	3.449912 ± 0.000009
ω_A (deg)	65.4 ± 0.6
$\dot{\omega}$ (deg century^{-1})	41 ± 16
T_o (HJD−2,400,000)[a]	54685.7012 ± 0.0003
i (deg)	87.19 (fixed)
U (years)	880 ± 250

Note. [a] Time of the deeper minimum.

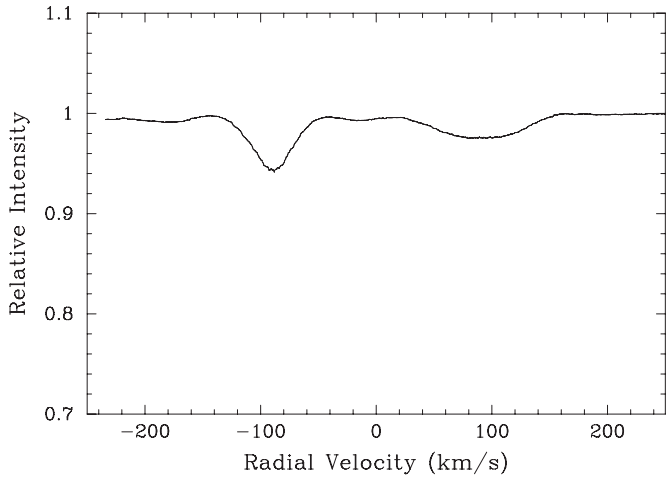

Figure 3. Average line profiles, summed from 36 spectral regions, of the V335 Ser components from a Fairborn Observatory spectrum. The primary is the blueshifted narrower lined star, while the secondary is the redshifted broader lined star.

State University (TSU) 2 m automatic spectroscopic telescope, a fiber-fed echelle spectrograph, and a 2048 × 4096 SITe ST-002A CCD (Eaton & Williamson 2007). The echelle spectrograms have 21 orders that cover the wavelength range 4920–7100 Å. The resolution depended on the fiber used and was either 0.24 or 0.4 Å, which produced typical signal-to-noise ratios of 60 and 100, respectively, at 6000 Å. The mean spectral profiles are shown in Figure 3.

In 2010 June, a single spectrum was obtained with the Kitt Peak National Observatory (KPNO) coudé feed telescope, coudé spectrograph, and a TI CCD. That spectrum is centered at 6430 Å, covers a wavelength range of 84 Å, and has a resolution of 0.21 Å or a resolving power of just over 30,000. The signal-to-noise ratio is about 150.

Fekel et al. (2009) have provided a general description of the velocity measurement for the Fairborn Observatory echelle spectra. However, because of its early spectral class, instead of a solar line list we have used a line list for V335 Ser that consists mostly of the lines of singly ionized elements such as Fe II, Si II, Ti II, and Cr II, which are prominent features in A and early-F stars. In addition, because the lines have moderately large rotational velocities, we have fitted the lines with rotationally broadened profiles (Lacy & Fekel 2011). The resulting velocities are on an absolute scale. Our unpublished measurements of several IAU solar-type velocity standards indicate that the Fairborn Observatory velocities have a small zero-point offset of -0.3 km s^{-1} relative to the velocities of Scarfe (2010). Thus, we have added 0.3 km s^{-1} to each Fairborn velocity. The radial velocity observations in Table 3 and fitted orbit are shown in Figure 4.

Adopting the photometric period, preliminary orbital elements of the primary were determined with BISP, a computer program that uses the Wilsing–Russell method to obtain preliminary orbital elements (Wolfe et al. 1967). Separate orbits for the primary and secondary were then computed with SB1 (Barker et al. 1967), a program that uses differential corrections to determine improved orbital elements. From the variances of the two solutions the velocities of the primary and secondary were assigned weights of 1.0 and 0.1, respectively. The center-of-mass velocities of the two solutions are in excellent accord, differing by only 0.3 km s^{-1}, a 1σ result. The other orbital elements that are common to both components also are in good agreement.

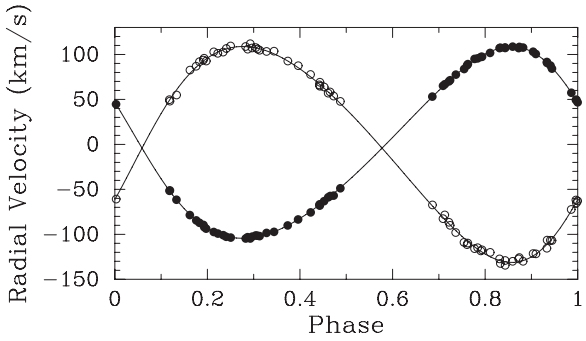

Figure 4. TSU radial velocities and fitted orbit for V335 Ser. Filled and open circles represent the primary (more massive star) and secondary (less massive star), respectively. In this diagram, zero phase is a time of periastron passage.

Thus, we combined the appropriately weighted velocities of the two components into a double-lined solution, using a slightly modified version of SB1. The resulting orbital elements and related parameters are given in Table 4. We also computed a double-lined solution with the period as a free parameter. The result is $P = 3.4498768 \pm 0.0000206$ days, a value in excellent accord with the more accurate photometrically determined value of 3.4498837 ± 0.0000012 days. The radial velocities are compared with the computed velocity curves in Figure 4. In this diagram, zero phase is a time of periastron. The time of conjunction with the more massive star behind, which corresponds to a primary eclipse, occurs at a spectroscopic phase of 0.052.

From the 12 Fairborn Observatory spectra with the highest signal-to-noise ratios, the rotational broadening fits result in average $v \sin i$ values of 30 ± 2 and 51 ± 3 km s^{-1} for components A and B, respectively. The uncertainties for the projected rotational velocities are conservative estimates. From those same spectra the average equivalent width ratio of the secondary relative to the primary, for lines centered at about 5540 Å, is 0.70 ± 0.02.

Spectra of a variety of early- and mid-A stars of known spectral type were rotationally broadened, shifted in wavelength space, and added together (Barden 1985) to reproduce the KPNO spectrum of V335 Ser in the 6430 Å region. The star 68 Tau is a known early-type Am star with an effective temperature of 9000 K (Pintado & Adelman 2003), and its spectrum appears to be a reasonably good fit to that of the primary. The lines of the secondary are broader and weaker, making a comparison more uncertain than for the primary, but an acceptable fit was found with HR 7502 which is a somewhat cooler mid-A star, as indicated by its Hβ value of 2.812 (Crawford et al. 1966). Thus, we conclude that the primary is an early-type Am star and the secondary is a mid-A type star. Because of the metallic-lined nature of the spectrum, we do not expect the equivalent width ratio given above to be equal to the visual light ratio determined from the light curves in Section 5.3 below.

5. PHOTOMETRIC OBSERVATIONS AND ORBIT

5.1. Interstellar Reddening and Mean Temperature

Color indices in the *uvbyβ* photometric system have been published by Knude (1981) based on three sets of measurements. This photometric system is designed to allow accurate estimation of the interstellar reddening. The β value and spectral type place the mean spectral type in the A star region. The *uvbyβ* indices indicate that the mean spectral type is A2 according to Popper's (1980) Table 1. Following the precepts of Glaspey (1972), we find an interstellar reddening value of

Table 3
Radial Velocity Observations from the TSU and Residuals from the Fitted Orbit

HJD−2,400,000	Phase After Periastron	RV_A (km s^{-1})	$(O-C)_A$ (km s^{-1})	RV_B (km s^{-1})	$(O-C)_B$ (km s^{-1})
55247.007	0.754	83.7	−1.1	−109.0	−4.7
55254.008	0.784	95.7	0.1	−114.8	1.7
55258.012	0.944	84.3	−1.1	−106.9	−1.9
55259.012	0.234	−100.9	0.2	102.7	−2.5
55268.013	0.843	107.3	−0.9	−129.1	1.5
55269.013	0.133	−61.5	0.0	54.8	−5.7
55270.013	0.423	−75.7	−1.3	77.7	2.6
55271.013	0.713	66.8	0.5	−78.5	4.9
55272.013	0.003	44.8	0.3	−60.8	−1.9
55273.013	0.293	−104.7	−0.8	112.0	3.7
55275.013	0.872	107.1	−1.0	−127.4	3.2
55276.013	0.162	−78.6	−0.7	82.7	3.7
55277.013	0.452	−63.2	0.1	63.9	1.4
55282.984	0.183	−87.2	−0.2	91.9	2.6
55283.984	0.473	−57.0	−2.4	53.7	0.9
55284.984	0.763	89.3	1.3	−109.7	−1.7
55286.934	0.328	−98.5	1.6	103.4	−0.6
55289.934	0.197	−93.6	−1.3	92.7	−2.5
55290.934	0.487	−48.8	−0.6	47.7	2.2
55291.934	0.777	95.0	1.6	−115.9	−1.9
55295.949	0.941	87.6	0.4	−106.6	0.4
55296.759	0.176	−84.6	−0.5	86.9	0.9
55298.778	0.761	87.9	0.5	−111.5	−4.2
55300.789	0.344	−97.3	−0.1	103.6	2.9
55303.916	0.250	−103.6	−0.4	109.5	2.0
55312.826	0.833	107.5	0.4	−132.3	−2.8
55313.809	0.118	−51.7	−0.3	49.8	0.6
55317.842	0.287	−103.1	1.1	105.9	−2.7
55319.761	0.843	107.7	−0.5	−134.5	−3.9
55324.775	0.297	−102.6	1.1	107.2	−0.9
55326.869	0.904	103.1	0.7	−121.4	2.7
55327.862	0.191	−89.5	0.7	93.8	0.9
55334.869	0.223	−99.1	−0.1	101.3	−1.4
55338.918	0.396	−83.5	0.0	87.5	2.2
55359.779	0.443	−66.6	0.3	64.7	−1.9
55362.764	0.308	−101.5	1.2	106.0	−0.9
55366.755	0.465	−57.4	0.5	58.3	1.9
55374.787	0.793	97.4	−1.2	−117.2	2.6
55381.747	0.811	101.8	−1.3	−120.0	5.0
55385.802	0.986	57.5	−0.2	−72.4	1.3
55412.727	0.791	97.3	−0.5	−118.4	0.6
55576.004	0.119	−51.1	1.1	48.1	−1.9
55584.021	0.443	−68.0	−1.1	69.1	2.5
55615.909	0.686	53.1	0.1	−67.3	1.2
55623.882	0.997	49.6	0.6	−65.2	−1.2
55631.842	0.305	−101.3	1.8	107.7	0.4
55638.980	0.374	−90.1	0.0	92.7	−0.1
55659.915	0.442	−67.5	−0.2	66.2	−0.9
55664.805	0.859	108.7	0.0	−130.1	1.2
55667.789	0.724	71.3	−0.4	−90.0	−0.5
55671.783	0.882	107.6	0.6	−129.9	−0.6
55673.780	0.461	−58.9	0.7	57.0	−1.4
55678.860	0.933	91.6	0.6	−115.4	−4.1
55679.827	0.214	−97.4	−0.5	102.9	2.5
55686.820	0.241	−102.7	−0.6	106.7	0.4
55692.889	1.000	46.7	−0.1	−62.9	−1.4
55695.757	0.831	107.1	0.2	−127.3	1.9
55698.829	0.722	70.0	−0.5	−86.6	1.6
55702.927	0.910	100.5	−0.1	−121.7	0.4
55703.905	0.193	−92.0	−1.2	95.8	2.3
55706.675	0.996	49.4	−0.6	−61.8	3.3
55712.680	0.737	77.5	0.2	−98.0	−2.2
55716.810	0.934	90.7	−0.1	−106.4	4.7
55729.834	0.709	65.2	0.8	−82.6	−1.3
55731.813	0.283	−104.7	−0.4	108.9	0.1
55733.853	0.874	108.4	0.4	−125.8	4.6
55738.817	0.313	−102.0	0.2	104.7	−1.7

Table 4
Spectroscopic Orbital Parameters

Parameter	Value	
	Star A	Star B
P^a (days)	3.4498837 (adopted)	
T (HJD periastron)	2455492.7960 ± 0.0052	
e	0.1411 ± 0.0013	
ω_A (deg)	65.28 ± 0.57	
K (km s^{-1})	106.57 ± 0.12	120.07 ± 0.38
γ (km s^{-1})	−4.12 ± 0.10	
Standard error (km s^{-1})	0.8	2.5
Observations	67	67

Note. [a] Photometric period.

$E(b-y) = 0.050 \pm 0.005$ mag, where the reddening uncertainty is based on the observational errors in the color indices, and a visual absorption of $A_v = 0.215$ mag. The value of δm_1 is not well determined for stars in this spectral range, so we cannot estimate the metallicity accurately from the photometry. The temperature calibration of Popper (1980), which is based primarily on that of Hayes (1978), gives a mean value of 8830 ± 150 K based on the value of $(b-y)_o$. The difference in the temperatures of the hotter and cooler components, $T_h - T_c$, is much more accurately known from the central surface brightness parameter J_B/J_A (see below) as 512 ± 30 K, following the method of Lacy (1987).

5.2. Differential Photometry

One of the telescopes used to obtain the differential photometry is the URSA WebScope, which consists of a Meade 10 inch f/6.3 LX-200 telescope with a Santa Barbara Instruments Group ST8 CCD camera (binned 2 × 2 to produce 765 × 510 pixel images with 2.3 arcsec square pixels) inside a Technical Innovations Robo-Dome, and controlled automatically by an Apple Macintosh G4 computer. The observatory is located on top of Kimpel Hall on the Fayetteville campus, with the control room directly beneath the observatory inside the building. Five-second exposures through a Bessell V filter (2.0 mm of GG 495 and 3.0 mm of BG 39) were read out and downloaded to the control computer over a 30 s interval, then the next exposure was begun. The observing cadence was therefore about 35 s per observation. The variable star would frequently be monitored continuously for 2–6 hr. V335 Ser was observed by URSA on 60 nights during parts of three observing seasons from 2008 April 28 to 2012 January 29, yielding 7456 observations.

The other telescope we used is the NFO WebScope, a refurbished 24 inch Group 128 cassegrain reflector with a 2K × 2K Kodak CCD camera, located near Silver City, NM (Grauer et al. 2008). Observations consisted of 5 s exposures through a Bessell V filter. V335 Ser was observed by the NFO on 101 nights during parts of three observing seasons from 2008 April 11 to 2012 February 5, yielding 5666 observations.

The images were analyzed by a virtual measuring engine application written by Lacy that flat-fielded the URSA images (the NFO images are flat-fielded before distribution), automatically located the variable, comparison, and check stars in the image, measured their brightnesses, subtracted the corresponding sky brightness, and corrected for the differences in airmass between the stars. Extinction coefficients were determined nightly from the comparison star measurements. They averaged 0.25 mag airmass^{-1} at URSA (they ranged from 0.20 to 0.30 mag airmass^{-1}), 0.18 mag airmass^{-1} at the NFO (they ranged from 0.12 to 0.25 mag airmass^{-1}). The comparison stars were TYC 0366-0878-1 (HD 143395, $V = 7.19$, K5) and TYC 0353-1061-1 ($V = 9.88$, F2). Both comparison stars are within 20 arcmin of the variable star. The mean nightly comparison star magnitude differences were constant at the level of 0.019 mag (URSA) and 0.034 mag (NFO) for the standard deviation of the mean magnitude differences between nights, and 0.023 mag (URSA) and 0.018 mag (NFO) for the standard deviation of the nightly differential magnitudes within nights. For the differential magnitudes, the sum of the fluxes of both comparison stars was converted to a magnitude called "comparisons." The resulting 7456 (URSA) and 5666 (NFO) V magnitude differences (variable-comparisons) are listed in Tables 5 and 6 (without any nightly corrections) and are shown in Figures 5–7 (after the nightly corrections discussed below have been added).

Table 5
URSA Differential V Magnitudes of V335 Ser

Orbital Phase	ΔV (mag)	HJD−2,400,000
0.72058	0.297	54584.71395
0.72074	0.327	54584.71452
0.72090	0.282	54584.71507
0.72106	0.308	54584.71563
0.72122	0.300	54584.71619

(This table is available in its entirety in machine-readable and Virtual Observatory (VO) forms in the online journal. A portion is shown here for guidance regarding its form and content.)

Table 6
NFO Differential V Magnitudes of V335 Ser

Orbital Phase	ΔV (mag)	HJD−2,400,000
0.82677	0.251	54567.83082
0.82702	0.262	54567.83169
0.82728	0.261	54567.83260
0.82754	0.256	54567.83348
0.82779	0.263	54567.83435

(This table is available in its entirety in machine-readable and Virtual Observatory (VO) forms in the online journal. A portion is shown here for guidance regarding its form and content.)

5.3. Photometric Orbit

The light curve fitting was done with the NDE model as implemented in the code *JKTEBOP* (Etzel 1981; Popper & Etzel 1981; Southworth et al. 2007), and the linear eclipse ephemeris adopted is that of Section 2. The main adjustable parameters are the relative central surface brightness of the cooler star (J_B/J_A) in units of the central surface brightness of the hotter star, the sum of the relative radii of the cooler and hotter stars ($r_A + r_B$) in units of the separation, the ratio of radii ($k = r_B/r_A$), the inclination of the orbit (i), and the geometric factors e cos ω and e sin ω which account for the orbital eccentricity. Auxiliary parameters needed in the analysis include the gravity-brightening exponent, which we adopt as 1.00 and 0.97 for the hotter and cooler stars, respectively, based on their temperatures (Claret 1998). Linear-law limb-darkening coefficients of 0.54 and 0.58 were adopted from the tables of Díaz-Cordovés et al. (1995) based on the temperatures and surface gravities of the components.

The mass ratio ($q = M_B/M_A = 0.888$) was adopted from the spectroscopic analysis in Section 4. Other adjusted parameters

Table 7
Photometric Orbital Parameters for V335 Ser in the *V* Band

Parameter	URSA	NFO	Adopted
J_B/J_A	0.850 ± 0.003	0.850 ± 0.002	0.850 ± 0.003
$r_A + r_B = (R_A + R_B)/a$	0.2450 ± 0.0006	0.2460 ± 0.0005	0.2455 ± 0.0006
$r_A = R_A/a$	0.1323 ± 0.0017	0.1326 ± 0.0016	0.1325 ± 0.0017
$r_B = R_B/a$	0.1127 ± 0.0022	0.1135 ± 0.0018	0.1131 ± 0.0022
$k = r_A/r_B$	0.852 ± 0.031	0.856 ± 0.022	0.854 ± 0.031
i (deg)	87.19 ± 0.15	87.19 ± 0.10	87.19 ± 0.15
e	0.1392 ± 0.0020	0.1404 ± 0.0015	0.1400 ± 0.0020
ω_A (deg)	64.8 ± 0.4	65.1 ± 0.3	65.0 ± 0.4
u_A (linear)	0.54 fixed	0.54 fixed	
u_B (linear)	0.58 fixed	0.58 fixed	
y_A	1.00 fixed	1.00 fixed	
y_B	0.97 fixed	0.97 fixed	
$q = m_A/m_B$	0.888 fixed	0.888 fixed	
L_A	0.619 ± 0.016	0.617 ± 0.012	0.618 ± 0.016
L_B	0.375 ± 0.016	0.377 ± 0.012	0.376 ± 0.016
$L_B/(L_A + L_B)$	0.60 ± 0.04	0.61 ± 0.03	0.61 ± 0.04
L_3	0 fixed	0 fixed	
σ (mmag)	14.488010	9.699360	
N	7456	5666	
Corrections	60	132	

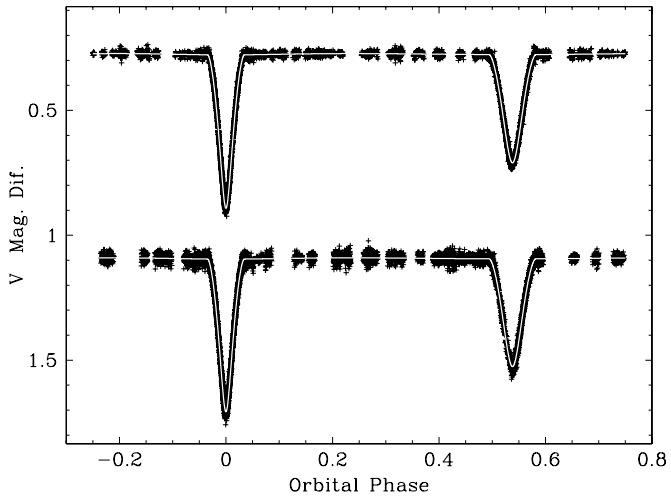

Figure 5. Visual-band light curves of V335 Ser from the NFO (top) and URSA (bottom) WebScopes, shifted vertically by an arbitrary amount for clarity. The white curves are the fitted photometric orbits.

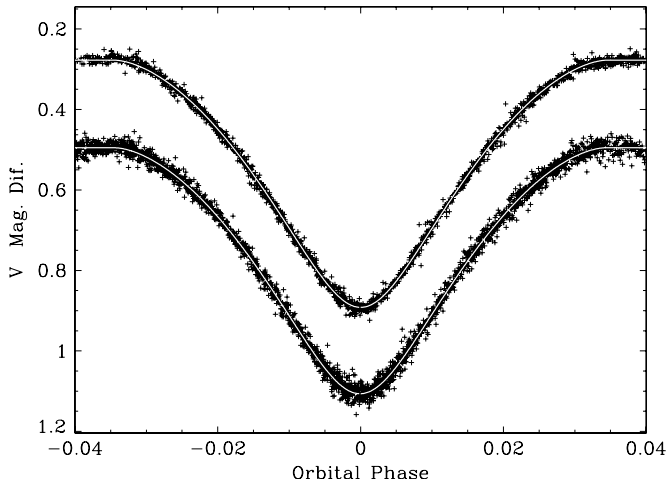

Figure 6. Visual-band light curves of V335 Ser at primary eclipse from the NFO (top) and URSA (bottom) WebScopes, shifted vertically by an arbitrary amount for clarity. The white curves are the fitted photometric orbits.

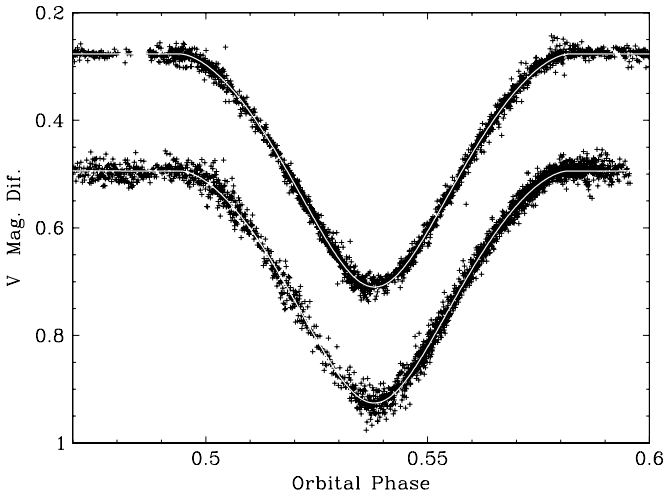

Figure 7. Visual-band light curves of V335 Ser at secondary eclipse from the NFO (top) and URSA (bottom) WebScopes, shifted vertically by an arbitrary amount for clarity. The white curves are the fitted photometric orbits.

were the magnitude at quadrature and the phase of the deeper eclipse. The amount of "reflected light" was calculated from bolometric theory (see Popper & Etzel 1981). The fitting procedure converged to very similar solutions for the separately analyzed URSA and NFO data sets (Table 7).

Examination of the residuals showed that small but significant night-to-night residual variations remained in the NFO data even after application of the photometric flat, and to a much smaller extent, were also present in the URSA data. The fact that they are essentially absent from the URSA data, which were obtained contemporaneously with the NFO data, shows that they are not intrinsic variations in the stars' brightness, but are only optical effects due to the type of telescope used. We have applied nightly corrections, based on the initial photometric orbits, to the data sets to remove these observational effects. The number of nights on which these adjustments were made is listed in Table 7 as "Corrections." Fits to the "corrected" data then show significantly reduced residual variance, and we have adopted these improved fits for further use.

Table 8
Absolute Properties of V335 Ser

Parameter	Star A[a]	Star B
Mass (solar masses)	2.147 ± 0.014	1.906 ± 0.008
Radius (solar radii)	2.03 ± 0.03	1.73 ± 0.04
log g (cm s^{-2})	4.155 ± 0.011	4.241 ± 0.017
Eccentricity e[b]	0.1408 ± 0.0009	
$v \sin i$ (km s^{-1}) (observed value)	30 ± 2	51 ± 3
Circular $v_{\rm sync}$ (km s^{-1}) (equatorial)	29.8	25.4
Pseudosynchronous $v_{\rm sync}$ (km s^{-1}) from Hut (1981)	28.4	33.3
Orbital semi-major axis a (solar radii)	15.324 ± 0.028	
$T_{\rm eff}$ (K)	9020 ± 150	8510 ± 150
log L (solar units)	1.39 ± 0.03	1.15 ± 0.04
M_V (mag)	1.27 ± 0.05	1.82 ± 0.06
F_V	3.945 ± 0.004	3.924 ± 0.004
E_{b-y} reddening (mag)	0.050 ± 0.005	
$m - M$ (mag)	6.48 ± 0.10	
Distance (pc)	197 ± 10	

Notes.
[a] The primary star A is the more massive one, which is larger and hotter than the secondary star B.
[b] This is a weighted value determined from the analysis of dates of minima, radial velocities, and differential photometry.

Residuals from the fits were checked for periodic variations by using the Mac.Period application (Lacy 1993). No sign of periodic variations were seen for periods ranging from 0.1 to 100 days.

The uncertainties of the fitted parameters of the light curve solutions were estimated by the jktebop method and also checked by doing 500 Monte Carlo simulations of the light curve data, which confirmed the essential correctness of the initial error estimates.

Nonlinear limb-darkening laws were tested to see if they would improve the fits. The quadratic laws of Claret (2000) and Claret & Hauschildt (2003) were tried, but they did not improve the fit, so the linear laws we used were the best fits to the data.

6. COMPARISON WITH THEORY

Combination of the fitted radial velocity parameters, the fitted ephemeris curve solution, and the fitted photometric orbit gives the absolute properties of Table 8. The masses are accurate to better than 0.7% and the radii to better than 2%. These absolute properties have been compared with the predictions of the Yonsei–Yale models (Yi et al. 2001) and the Granada models (Claret 2004). Figure 8 shows the observed and theoretical Yonsei–Yale main sequence with an isochrone for an age of 370 Myr and with a metallicity of $Z = 0.0189$. The observed properties fit the theoretical main sequence well, but there is relatively poor agreement on the age of the system (±60 Myr). Similar results are found from a comparison with the Granada models at an age of 380 Myr with a metallicity of $Z = 0.020$.

Because the apsidal motion has been accurately measured in Section 3 above, a comparison between the observed internal structure constant and the theoretical prediction of the Granada models can be made. Here we have corrected for the rotational distortions and the relativistic contribution as in Giménez (1985) to find the mean Newtonian structure constant, log k_2. The theoretical result is log $k_2 = -2.44 \pm 0.08$ and the observational result is -2.13 ± 0.17, so they do not agree. It is known that disagreements of this sort can occur if the rotation axes of the stars and the orbital axis are misaligned, as in the famous case of DI Her (Albrecht et al. 2009), so that may be a plausible explanation. It would take additional spectroscopic observations to test this hypothesis.

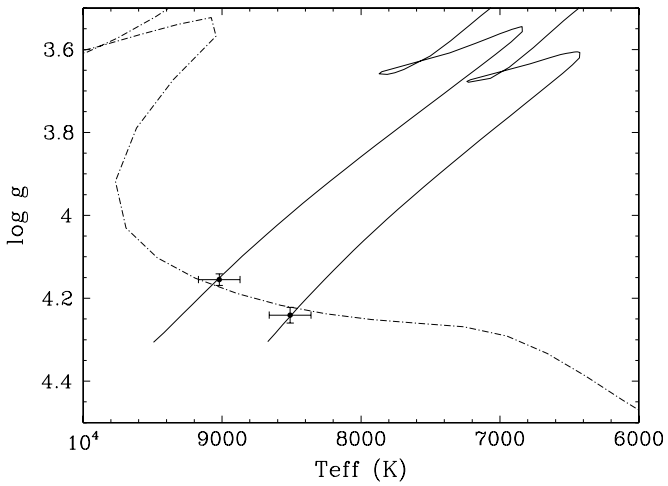

Figure 8. Observed properties (dots with error bars), evolutionary tracks (solid curves), and an isochrone (dot-dashed curve) for an age of 370 Myr ($Z = 0.0189$) according to the models by Yi et al. (2001).

The theoretical timescales for orbital circularization and spin synchronization may be computed from the Granada models. The time for orbital circularization in years is log $t_{\rm cir} = 8.70$, slightly greater than the system age (log $t = 8.57 \pm 0.06$), so is not inconsistent with the observed eccentric orbit. The theoretical spin synchronization times, however, are slightly less than the system age (8.51 and 8.53), which is contrary to the observed asynchronous spin of star B (star A is spinning synchronous with the mean angular rate, and star B is spinning at twice the mean angular rate). Such disagreements between theory and observation of binary star spin states are not uncommon (see Lacy et al. 2012).

7. COMPARISON WITH THE WORK OF BOZKURT (2011)

Bozkurt (2011) was the first to publish absolute properties of this eclipsing binary, but his work is based on many fewer

Table 9
Comparison of Results to Prior Work

	Bozkurt (2011)[a]	This Paper[a]
Primary orbital period (days)	3.4498772(25)	3.4498837(12)
Eccentricity	0.1379(6)	0.1408(9)
Longitude of periastron (deg)	63.49(12)	65.2(4)
Apsidal period (years)	261.15(51397)	880(250)
r_A	0.1354(2)	0.1325(17)
r_B	0.1065(1)	0.1131(22)
i (deg)	87.83(3)	87.19(15)
T_A (K)	9500	9020(150)
T_B (K)	8885(5)	8510(150)
γ (km s^{-1})	−5.97(52)	-4.12(10)
L_A (V)	0.665(2)	0.61816)
L_B (V)	0.345	0.376(16)
K_A (km s^{-1})	106.31(88)	106.57(12)
K_B (km s^{-1})	116.94(88)	120.07(38)
M_A (solar masses)	2.02(1)	2.147(14)
M_B (solar masses)	1.84(2)	1.906(8)
R_A (solar radii)	2.03(2)	2.03(3)
R_B (solar radii)	1.60(1)	1.73(4)
log g_A (cgs)	4.128(9)	4.155(11)
log g_B (cgs)	4.295(7)	4.241(17)
log luminosity (A) (solar units)	1.479(35)	1.39(3)
log luminosity (B) (solar units)	1.156(43)	1.15(4)
Distance (pc)	219(24)	197(10)

Note. [a] The values in parentheses are the standard errors in units of the last decimal place.

observations than ours. He had 763 differential photometric observations in each of two filters, whereas we have 7456 + 5666 differential photometric observations from two independent telescopes. He had 12 spectroscopic observations whereas we have 67. A comparison of his results with ours is given in Table 9. In many cases the results are significantly different, such as the 6% difference in r_B, the 6% difference in m_A, and the very different values of L_A/L_B (15% difference). We believe that the differences are mainly due to the smaller number of Bozkurt's observations.

The authors thank Bill Neely who operates and maintains the NFO WebScope for the Consortium, and who handles preliminary processing of the images and their distribution. The authors also thank the staff at KPNO, especially Daryl Willmarth, for maintenance and preparation of the coudé-feed telescope and spectrometer.

REFERENCES

Albrecht, S., Reffert, S., Snellen, I. A. G., & Winn, J. N. 2009, Nature, 461, 373
Agerer, F., & Hübscher, J. 2002, IBVS, 5296
Barden, S. C. 1985, ApJ, 295, 162
Barker, E. S., Evans, D. S., & Laing, J. D. 1967, R. Obs. Bull., 130, 355
Bastian, U., & Born, E. 1997, IBVS, 4536
Bastian, U., & Born, E. 1998, IBVS, 4590
Bozkurt, Z. 2011, New Astron., 16, 412
Brat, L., Smelcer, L., Kucakova, H., et al. 2008, Open Eur. J. Var. Stars, 94, 1
Claret, A. 1998, A&AS, 131, 395
Claret, A. 2000, A&A, 363, 1081
Claret, A. 2004, A&A, 424, 919
Claret, A., & Hauschildt, P. H. 2003, A&A, 412, 241
Crawford, D. L., Barnes, J. V., Faure, B. Q., Golson, J. C., & Perry, C. L. 1966, AJ, 71, 709
Díaz-Cordovés, J., Claret, A., & Giménez, A. 1995, A&AS, 110, 329
Eaton, J. A., & Williamson, M. H. 2007, PASP, 119, 886
Etzel, P. B. 1981, in Photometric and Spectroscopic Binary Systems, ed. C. B. Carling & E. Z. Kopal (Dordrecht: Reidel), 111
Fekel, F. C., Tomkin, J., & Williamson, M. H. 2009, AJ, 137, 3900
Giménez, A. 1985, ApJ, 297, 405
Glaspey, J. W. 1972, AJ, 77, 474
Grauer, A. D., Neely, A. W., & Lacy, C. H. S. 2008, PASP, 120, 992
Hayes, D. S. 1978, in IAU Symp. 80, The HR Diagram, ed. A. G. D. Philip & D. S. Hayes (Dordrecht: Reidel), 65
Hut, P. 1981, A&A, 99, 126
Knude, J. 1981, A&AS, 44, 225
Lacy, C. H. S. 1987, AJ, 94, 1035
Lacy, C. H. S. 1992, AJ, 104, 2213
Lacy, C. H. S. 1993, BAAS, 25, 809
Lacy, C. H. S. 2009, IBVS, 5910
Lacy, C. H. S. 2011, IBVS, 5972
Lacy, C. H. S. 2012, IBVS, 6014
Lacy, C. H. S., & Fekel, F. C. 2011, AJ, 142, 185
Lacy, C. H. S., Torres, G., Fekel, F. C., Sabby, J. A., & Claret, A. 2012, AJ, 143, 129
Makarov, V., Bastian, U., Hoeg, E., Grossman, V., & Wicenec, A. 1994, IBVS, 4118
Paunzen, E., Duffee, B., Heiter, U., Kuschnig, R., & Weiss, W. W. 2001, A&A, 373, 625
Pintado, O. I., & Adelman, S. J. 2003, A&A, 406, 987
Popper, D. M. 1980, ARA&A, 18, 115
Popper, D. M., & Etzel, P. B. 1981, AJ, 86, 102
Scarfe, C. D. 2010, Observatory, 130, 214
Southworth, J, Bruntt, H., & Buzasi, D. L. 2007, A&A, 467, 1215
Torres, G., Andersen, J., & Giménez, A. 2010, A&ARv, 18, 67
Wolfe, R. H., Horak, H. G., & Storer, N. W. 1967, in Modern Astrophysics, ed. M. Hack (New York: Gordon & Breach), 251
Yi, S. K., Demarque, P., Kim, Y.-C., et al. 2001, ApJS, 136, 417